Geochemical Perspectives Letters

Halogen enrichment on the continental surface: a perspective from loess

P-Y. Han, R.L. Rudnick, Z-C. Hu, T. He, M.A. Marks, K. Chen

Supplementary Information

The Supplementary Information includes:

- Samples and Analytical Methods
- Tables S-1
- Figures S-1 to S-11
- Supplementary Information References

Samples and Analytical Methods

The 129 loess samples investigated in this study were collected from four continents: Europe (Germany and Switzerland), North America (United States), South America (Argentina), and Asia (Kazakhstan and China). The latitude and longitude of the loess sections, along with references to the original investigations of these units, are given in Table S-1 and plotted in Figure S-1. Data for major elements, rare earth elements (REEs), total organic carbon (TOC), and halogens are reported in this study.

Major Elements and REE Analyses

The samples were powdered in an agate mortar mill (RS200, Retsch, Germany) prior to analysis. Major element concentrations were determined by X-ray fluorescence (RIX2100, Japan) on fused glass disks at Northwest University in Xi'an, China. Reference materials BCR-2 (basalt, USGS) and GSR-3 (basalt, Chinese National Standard) indicate that precision and accuracy are better than 5 %. Rare earth elements were analysed by ICP-MS (Agilent 7900) after high-pressure acid digestion of samples in Teflon bombs at the State Key Laboratory of Geological Processes and Mineral Resources (GPMR), China University of Geosciences, Wuhan. About 50 mg of sample powder was weighed into a Teflon bomb, and then 1 ml of concentrated HNO_3 and 1 ml of concentrated HF were added. The sealed bomb was heated at 190 °C in the oven for 72 hours. After cooling, the solution was evaporated to dryness at ~120 °C. This was followed by adding 1 ml of concentrated HNO_3 and evaporating to dryness again. The resultant salt was re-dissolved by adding 1 ml of HNO_3, 1 ml of Milli-Q water (18.2 MΩ), and 1 ml of 1µg/ml In internal standard solution. The solution was then resealed and heated in the bomb at 190 °C for ~24 hours. The final solution was diluted to ~100 g with 2 %

HNO_3 for ICP-MS analysis. Total procedure blanks are below detection limits. The results for reference materials (BCR-2, BHVO-2, AGV-2, and SCo-1) agree well with the recommended values, within 10 % uncertainties. Results for the reference materials are in Park *et al.* (2012).

Total Organic Carbon Analysis

Organic C measurements were conducted at the State Key Laboratory of Biogeology and Environmental Geology, China University of Geosciences, Wuhan. About 2 g of powdered sample was acidified with 50 % HCl to remove inorganic carbon from carbonates. The residue was rinsed with deionised water to neutralise pH, then centrifuged and dried for 48 hours, before being analysed using the 902 T C–S analyser (Beijing Wanliandaxinke Instruments Co. Ltd.). Based on multiple analyses of AR-4007 (total carbon: 7.62 %, Alpha Resources Inc.), AR-4017 (total carbon: 0.50 ± 0.03 %, Alpha Resources Inc.) and B2152 (total carbon: 1.30 ± 0.09 %, Elemental Microanalysis Ltd.), TOC data are reported with a precision better than ± 0.1 %.

Halogen Analyses and Leaching Experiment

Halogen concentrations of loess are obtained using two different methods: (1) F-Cl-Br analysis by combustion ion chromatography analysis (C-IC) conducted at Fachbereich Geowissenschaften, Universität Tübingen, and (2) Cl-Br-I analysis by NH_4HF_2 digestion and ICPMS analysis (N-ICPMS) conducted at State Key Laboratory of Geological Processes and Mineral Resources, China University of Geosciences, Wuhan. More detailed descriptions of these two methods can be found in Han *et al*. (2023). Although Cl and Br are both analysed in the above two methods, the measured Cl and Br content in loess by C-IC are often 25-50 % lower than those obtained by N-ICPMS, which is consistent with the results obtained by Han *et al*. (2023) on glacial diamictites (Fig. S-2). This discrepancy could result from incomplete halogen recovery by pyrohydrolysis (*e.g.*, Marks *et al*., 2017; Kendrick *et al*., 2018; Han *et al*., 2023). Therefore, we used the F data from C-IC and the Cl, Br, I data from N-ICPMS in this paper to investigate the behaviour of halogens in loess (Table S-1 and Fig. 1).

Halogen leaching experiments were performed on 14 loess samples from various localities (five from Germany, one from the United States, one from Kazakhstan, and seven from China) at State Key Laboratory of Geological Processes and Mineral Resources, China University of Geosciences, Wuhan. For each sample, ~150 mg of sample powder was first mixed with 5 ml Milli-Q water (18.2 MΩ), then sonicated for 5 minutes using ultrasound, and subsequently centrifuged for 7 minutes in a centrifuge. The solid residue was then separated and dried in an oven at 50 ºC for 48 hours. Finally, the residual sample powders were dissolved and analysed for Cl-Br-I content using the above N-ICPMS method.

Supplementary Table

Table S-1 Major elements, total organic carbon (TOC), and rare earth elements of loess samples.

Table S-1 is available for download (.xlsx) from the online version of this article at https://doi.org/10.7185/geochemlet.2442.

Supplementary Figures

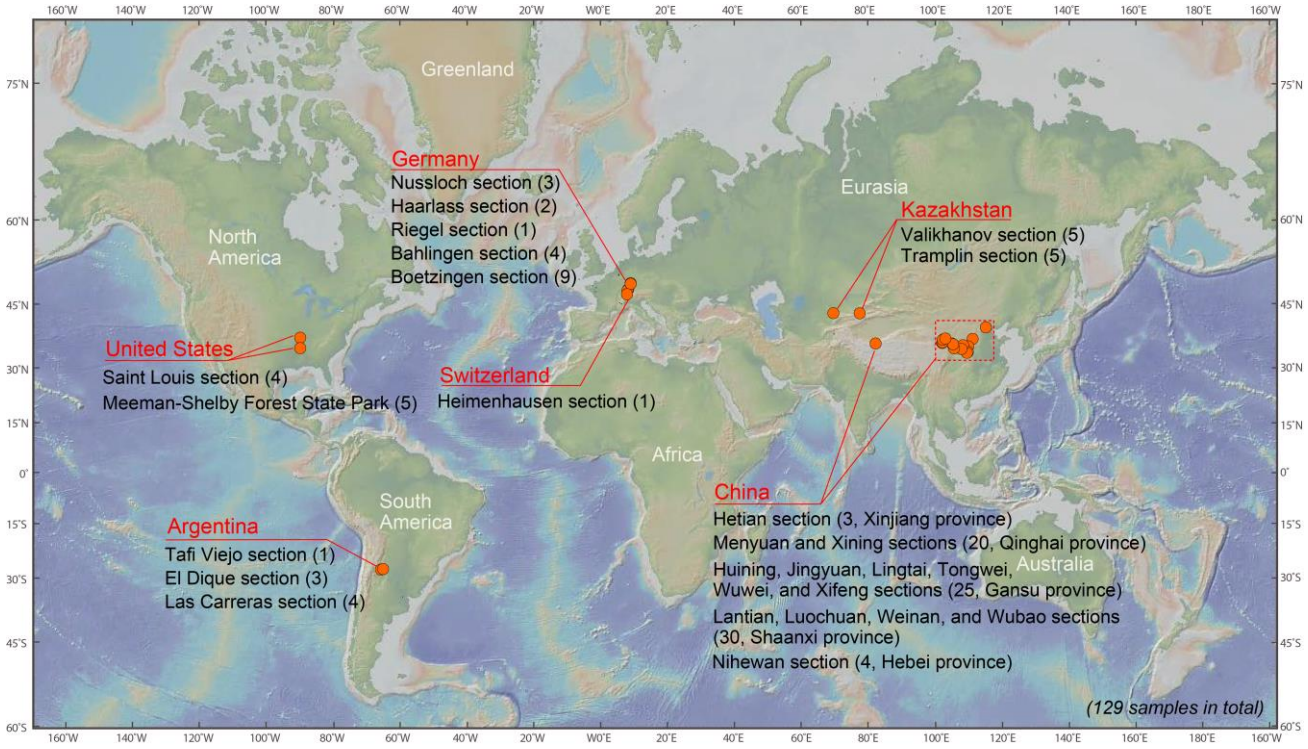

Figure S-1 Distribution of loess samples from this study. The number in parentheses indicates the quantity of samples analysed in each section.

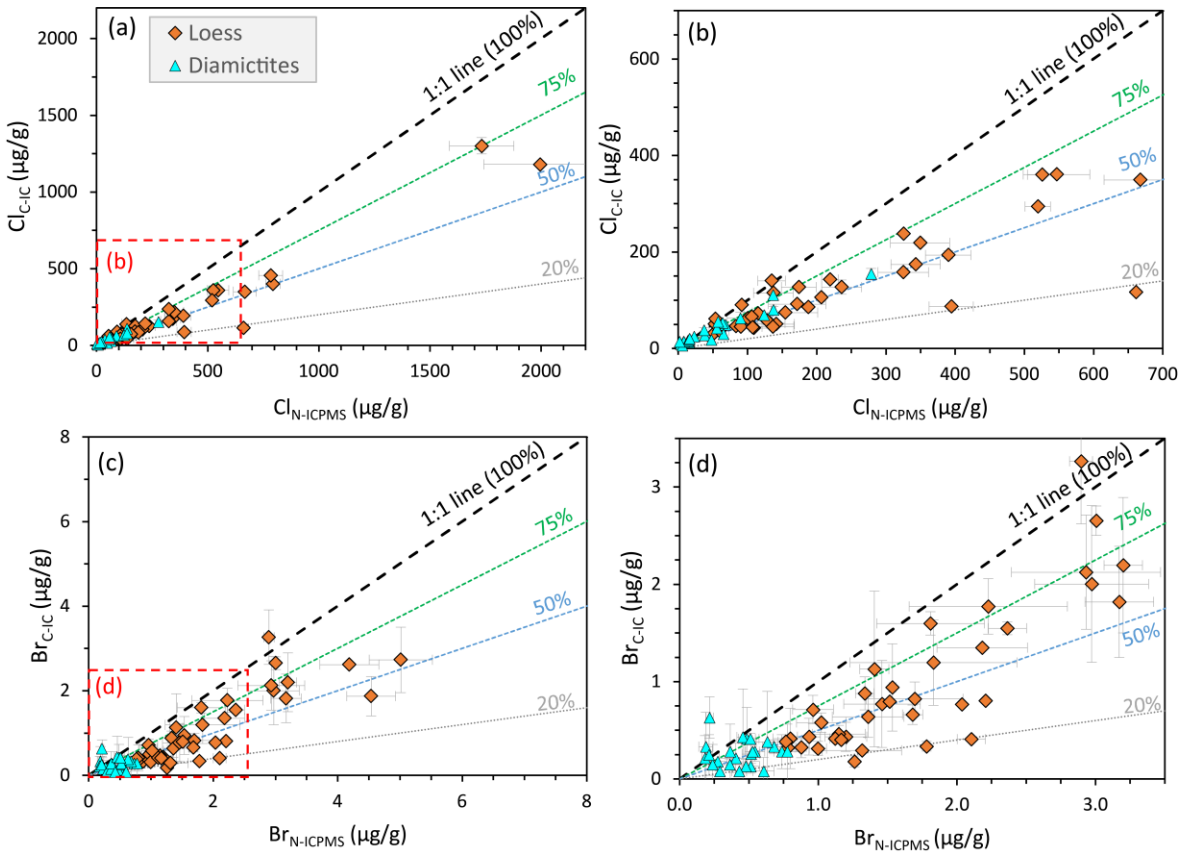

Figure S-2 Comparison of Cl **(a-b)** and Br **(c-d)** results for loess (this study) and glacial diamictite composites (Han *et al.*, 2023) by C-IC and N-ICPMS, respectively. Error bars represent 1σ.

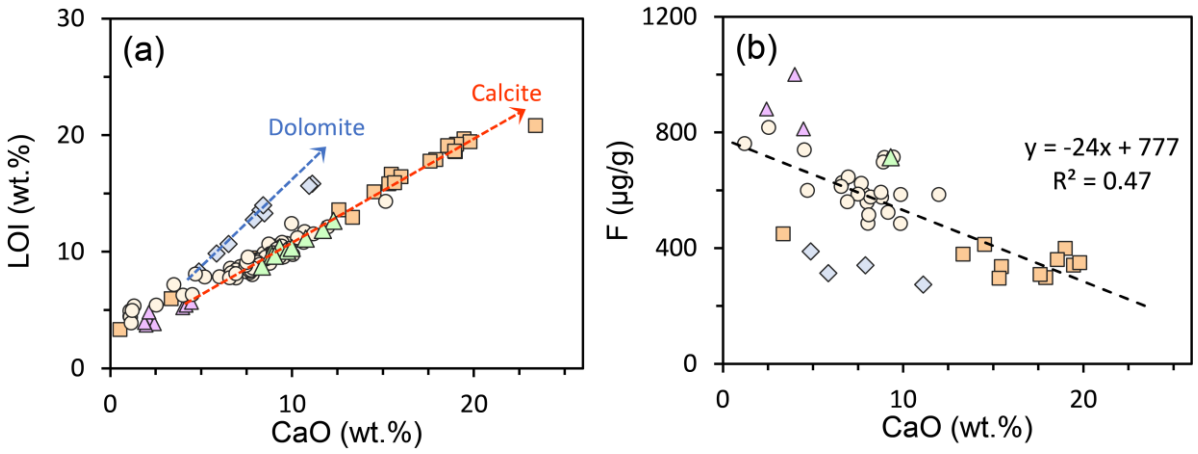

Figure S-3 **(a)** Loss of Ignition (LOI) of loess increases as the CaO content increases. The data follow the trends produced by having variable amounts of calcite (red-dashed line) and dolomite (blue dashed line) in the samples, suggesting that the CaO in loess is mainly controlled by carbonate. **(b)** Fluorine versus CaO content. There is a negative trend between F and CaO, likely due to the dilution of F content in loess samples by carbonate. Symbols as Fig. 2.

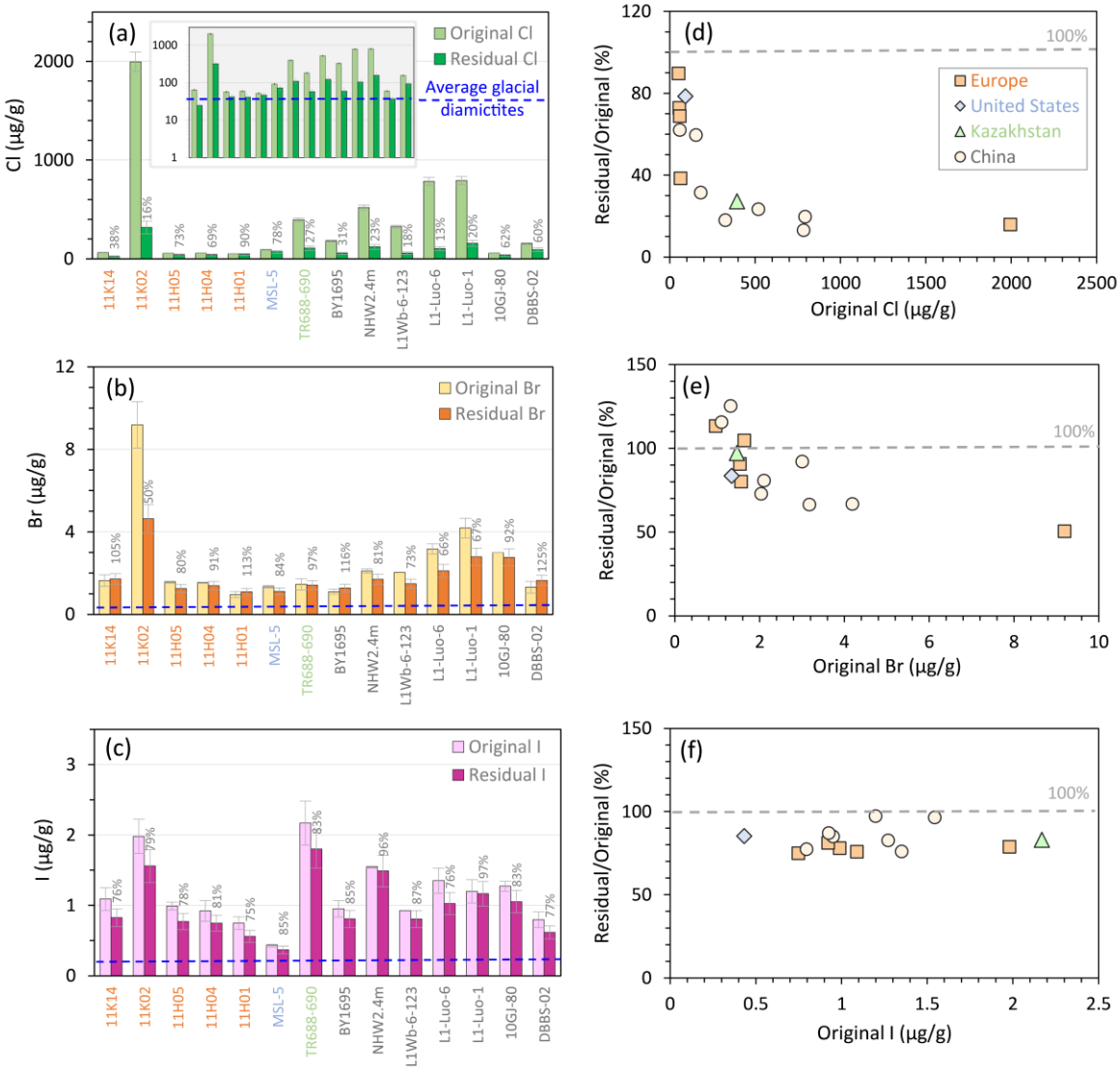

Figure S-4 Leaching experiments on loess samples for Cl, Br, and I. **(a-c)** show the Cl, Br, and I contents of the samples (on the x-axis) both before (original) and after (residual) leaching. The blue dashed lines represent the average Cl-Br-I content of glacial diamictites from Han et al. (2023). The inset figure in **(a)** is in log-scale. In **(d-f)**, the proportion of residual halogen components in the analysed loess samples (y-axis) is plotted against the original halogen concentrations (x-axis).

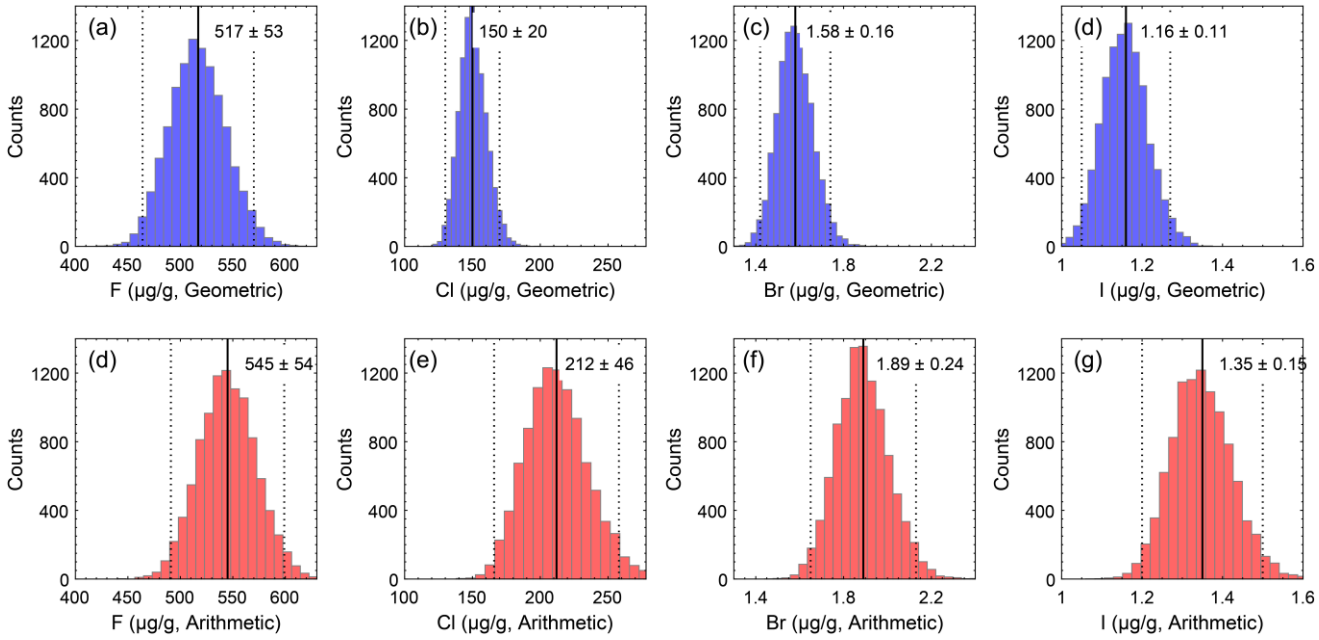

Figure S-5 Bootstrapped geometric **(a-d**, upper panel**)** and arithmetic **(d-g**, lower panel**)** means of loess F-Cl-Br-I data, which are computed using MATLAB, employing 10,000 trials. Each trial represents the geometric or arithmetic mean of a randomly resampled set of the loess data, with replacement allowed. The geometric/arithmetic means for the loess samples (Fig. 1) are determined by averaging the results of the 10,000 bootstrapped trials, shown as vertical black lines (2 standard errors indicated by black dashed lines). The arithmetic means consistently surpass the geometric means due to the skewed distribution of halogen concentrations in loess (Fig. 1).

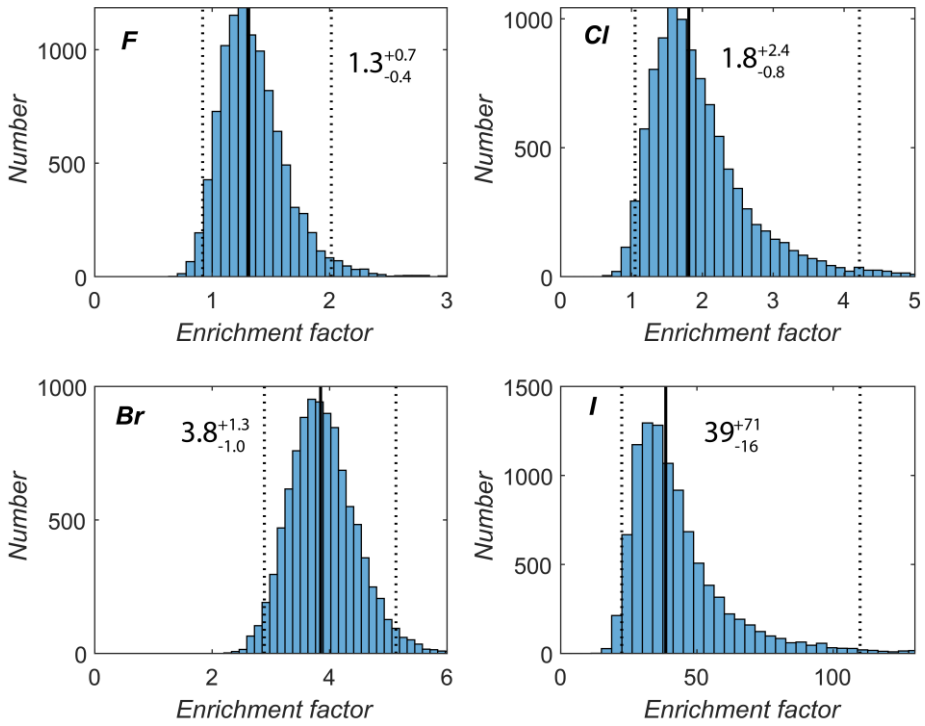

Figure S-6 Enrichment factor of halogens in loess relative to the estimates of the crystalline UCC (394 ± 67 µg/g F, 83 ± 24 µg/g Cl, 0.41 ± 0.04 µg/g Br, and 0.03 ± 0.01 µg/g I, with 2 standard deviations, from Han *et al.*, 2023), calculated by bootstrapping, with 10,000 trials. Each trial represents the median of randomly sampled loess compared to a random composition of the crystalline UCC within its 2 standard deviations. The black line represents the median of the 10,000 bootstrapped trials, and the dashed lines are 95 % confidence interval.

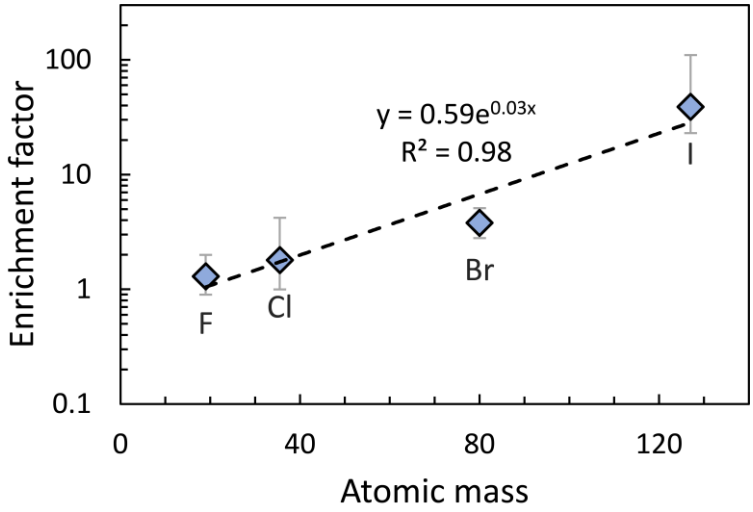

Figure S-7 The halogen enrichment factors in loess increase exponentially with their atomic masses. Error bars of halogen enrichment factors are at 95 % confidence level, see Figure S-6 for further details.

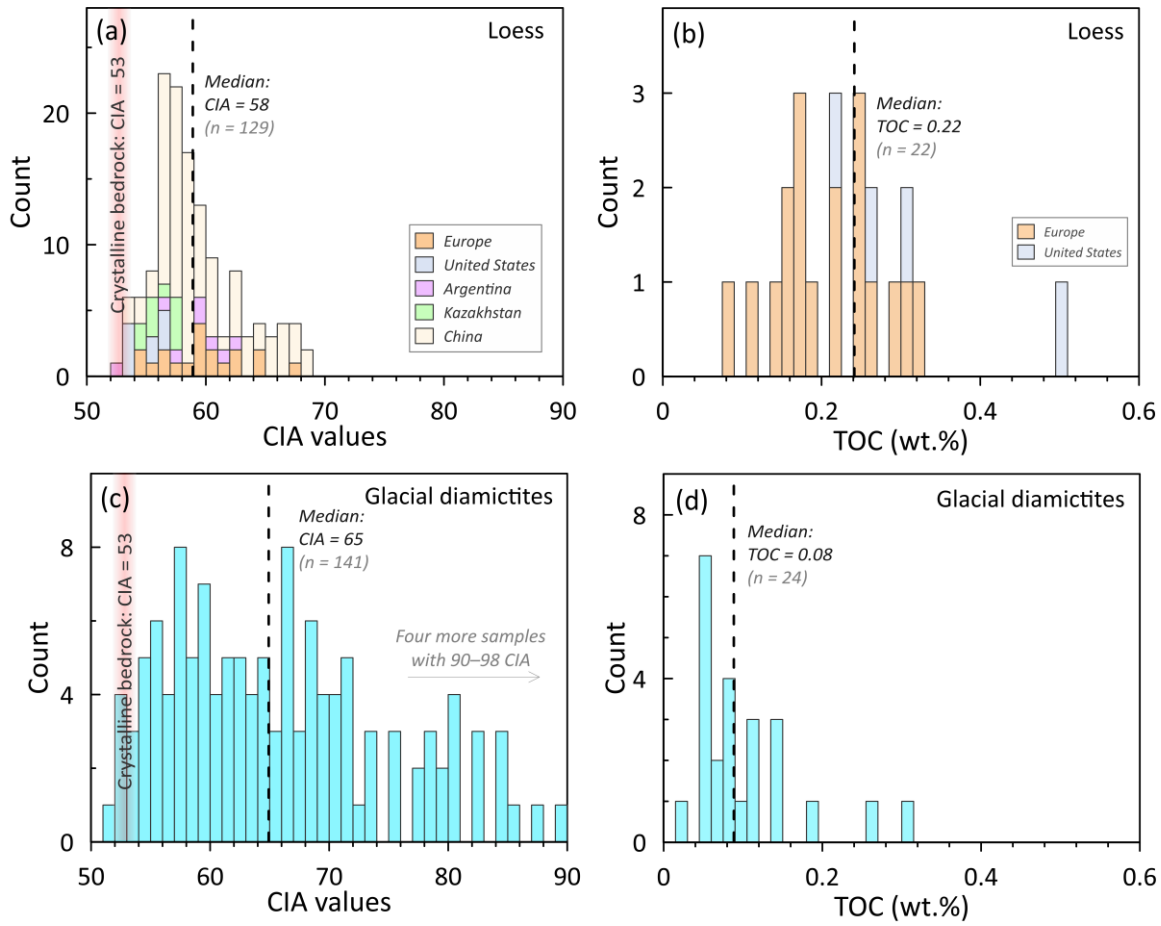

Figure S-8 Comparison of CIA value (chemical index of alteration, CIA = molar Al_2O_3 / (Al_2O_3 + CaO^*+ K_2O + Na_2O), where CaO^* is corrected for carbonate and apatite (Nesbitt and Young, 1982) and the carbonate correction is based on the approach of McLennan (1993), **a** and **c)** and TOC results **(b** and **d)** for loess (this study) and glacial diamictite composites, respectively. The CIA values of glacial diamictites are from Gaschnig *et al.* (2016) for 141 individual glacial diamictite samples, and the TOC data are from Greaney *et al.* (2020) for 24 glacial diamictite composites. The dashed line in each plot represents the median value for each population, and loess samples generally have limited and lower CIA values but higher TOC than glacial diamictites.

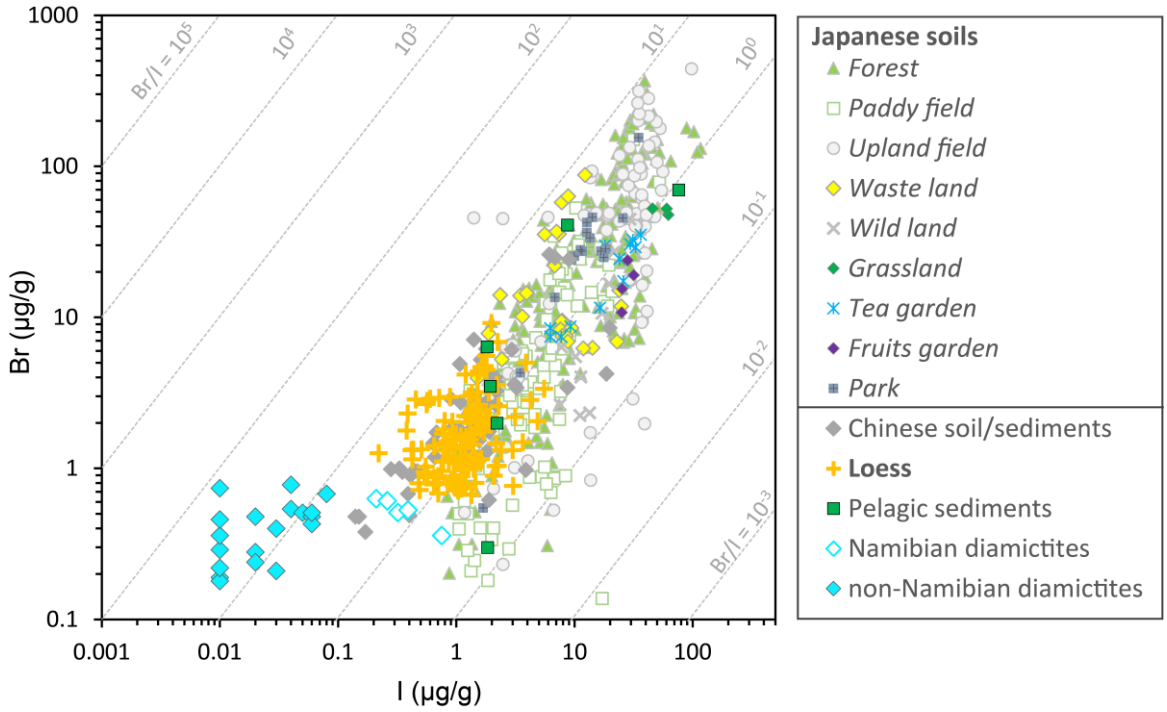

Figure S-9 Br versus I content of Japanese soils (Yamasaki *et al.*, 2015), Chinese soils/sediments (He *et al.*, 2018), loess (this study), pelagic sediments (John *et al.*, 2011), and glacial diamictites (Han et al., 2023). Within the glacial diamictite composites, five samples from Namibia exhibit notably elevated I content and relatively low Br/I ratios (the elevated I content of the Namibian samples is likely due to the presence of carbonate and abundant terrigenous sedimentary rocks in their provenance, see discussion in Han *et al.* (2023)).

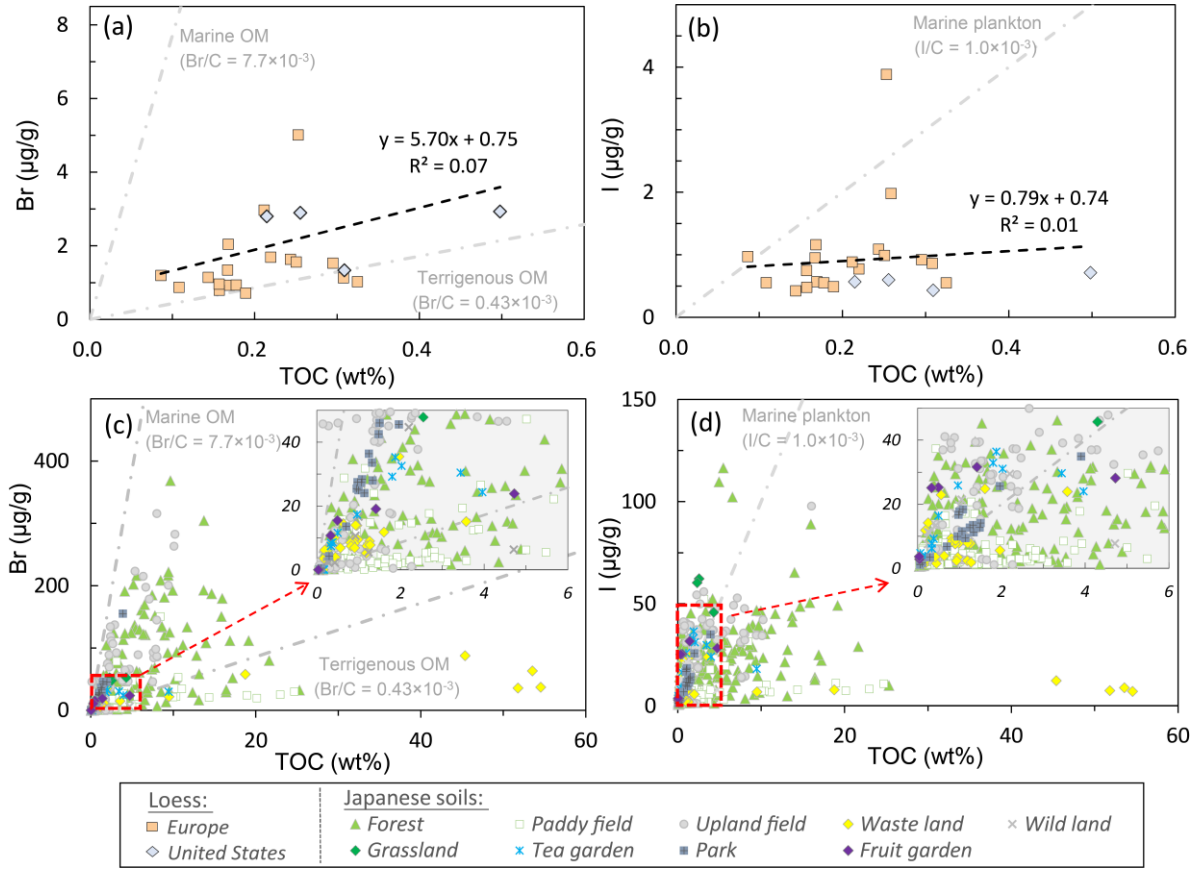

Figure S-10 Br and I versus TOC content of loess samples **(a-b**, this study**)** and Japanese soils **(c-d**, Yamasaki *et al.*, 2015**)**. In **(a)** and **(b)**, the correlation of Br and I with TOC of the analysed loess samples is indicated by the black dashed line, both showing very poor correlation (R^2 value ≤ 0.1). Br/C ratios for organic matter (OM) of terrigenous and marine sources ($0.43*10^{-3}$ and $7.7*10^{-3}$, respectively, from Mayer *et al.* (2007)) are plotted as grey dash-dotted lines in **(a)** and **(c)** for comparison. In b and d, the grey dash-dotted line represents the I/C ratio ($1.0*10^{-3}$) of typical marine plankton (Elderfield and Truesdale, 1980).

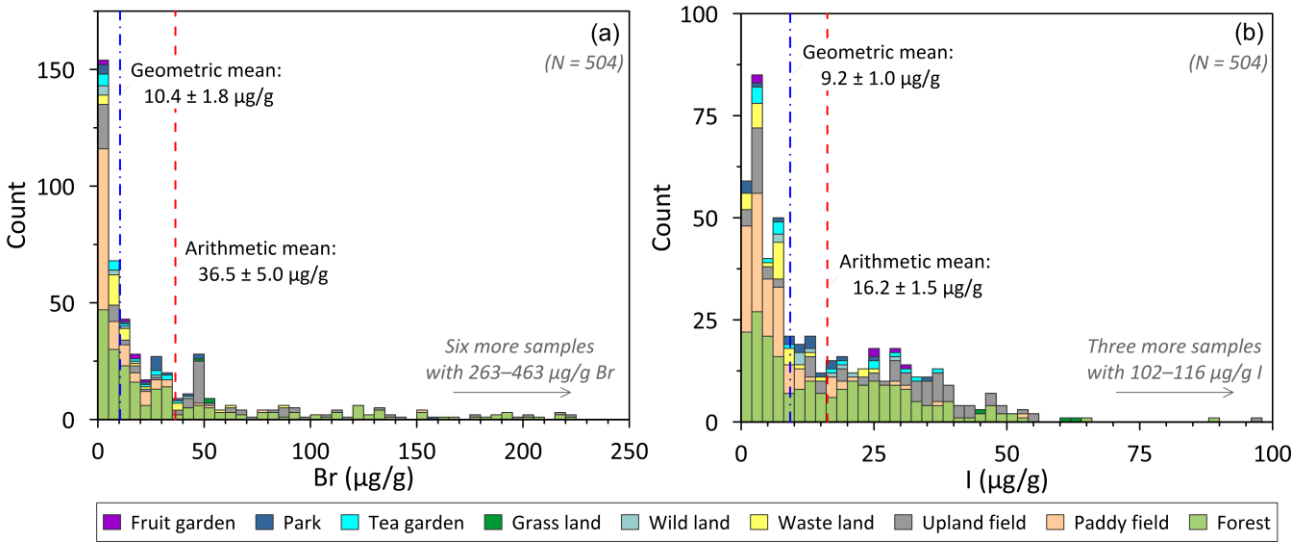

Figure S-11 Bromine and I content in various types of Japanese soil samples (Yamasaki *et al.*, 2015). The blue dash-dotted and the red dashed lines represent the geometric and arithmetic means of the dataset, respectively, along with 2 standard errors. Their calculations are the same as those for the loess data, see Figure S-5 for further details.

Supplementary Information References

Elderfield, H., Truesdale, V.W. (1980) On the biophilic nature of iodine in seawater. *Earth and Planetary Science Letters* 50, 105-114. https://doi.org/10.1016/0012-821X(80)90122-3

An, Z., Kukla, G.J., Porter, S.C., Xiao, J. (1991) Magnetic susceptibility evidence of monsoon variation on the Loess Plateau of central China during the last 130,000 years. *Quaternary Research* 36, 29-36. https://doi.org/10.1016/0033-5894(91)90015-W

Antoine, P., Rousseau, D.-D., Moine, O., Kunesch, S., Hatté, C., Lang, A., Tissoux, H., Zöller, L. (2009) Rapid and cyclic aeolian deposition during the Last Glacial in European loess: a high-resolution record from Nussloch, Germany. *Quaternary Science Reviews* 28, 2955-2973. https://doi.org/10.1016/j.quascirev.2009.08.001

Che, X., Li, G. (2013) Binary sources of loess on the Chinese Loess Plateau revealed by U–Pb ages of zircon. *Quaternary Research* 80, 545-551. https://doi.org/10.1016/j.yqres.2013.05.007

Derbyshire, E., Meng, X., Kemp, R.A. (1998) Provenance, transport and characteristics of modern aeolian dust in western Gansu Province, China, and interpretation of the Quaternary loess record. *Journal of arid environments* 39, 497-516. https://doi.org/10.1006/jare.1997.0369

Ding, Z., Ren, J., Yang, S., Liu, T. (1999) Climate instability during the penultimate glaciation: Evidence from two high-resolution loess records, China. *Journal of Geophysical Research: Solid Earth* 104, 20123-20132. https://doi.org/10.1029/1999JB900183

Feng, Z.-D., Ran, M., Yang, Q., Zhai, X., Wang, W., Zhang, X., Huang, C. (2011) Stratigraphies and chronologies of late Quaternary loess–paleosol sequences in the core area of the central Asian arid zone. *Quaternary International* 240, 156-166. https://doi.org/10.1016/j.quaint.2010.10.019

Gaschnig, R.M., Rudnick, R.L., McDonough, W.F., Kaufman, A.J., Valley, J.W., Hu, Z., Gao, S., Beck, M.L. (2016) Compositional of the upper continental crust through time, as constrained by ancient glacial diamictites. *Geochimica et Cosmochimica Acta* 186, 316-343. https://doi.org/10.1016/j.gca.2016.03.020

Greaney, A.T., Rudnick, R.L., Romaniello, S.J., Johnson, A.C., Gaschnig, R.M., Anbar, A.D. (2020) Molybdenum isotope fractionation in glacial diamictites tracks the onset of oxidative weathering of the continental crust. *Earth and Planetary Science Letters* 534, 116083. https://doi.org/10.1016/j.epsl.2020.116083

Guan, Q., Pan, B., Gao, H., Li, N., Zhang, H., Wang, J. (2008) Geochemical evidence of the Chinese loess provenance during the Late Pleistocene. *Palaeogeography, Palaeoclimatology, Palaeoecology* 270, 53-58. https://doi.org/10.1016/j.palaeo.2008.08.013

Guo, Z., Liu, T., An, Z. (1994) Paleosols of the last 0.15 Ma in the Weinan loess section and their paleoclimatic significance. *Quaternary Sciences* 14, 256-269.

Guo, Z., Biscaye, P., Wei, L., Chen, X., Peng, S., Liu, T. (2000) Summer monsoon variations over the l1.2 Ma from the weathering of loess-soil sequences in China. *Geophysical Research Letters* 27, 1751-1754. https://doi.org/10.1029/1999GL008419

Han, P.-Y., Rudnick, R.L., He, T., Marks, M.A., Wang, S.-J., Gaschnig, R.M., Hu, Z.-C. (2023) Halogen (F, Cl, Br, and I) concentrations of the upper continental crust through time as recorded in ancient glacial diamictite composites. *Geochimica et Cosmochimica Acta* 341, 28-45. https://doi.org/10.1016/j.gca.2022.11.012

He, T., Xie, J., Hu, Z., Liu, T., Zhang, W., Chen, H., Liu, Y., Zong, K., Li, M. (2018) A rapid acid digestion technique for the simultaneous determination of bromine and iodine in fifty-three Chinese soils and sediments by ICP-MS. *Geostandards and Geoanalytical Research* 42, 309-318. https://doi.org/10.1111/ggr.12212

Jahn, B.-m., Gallet, S., Han, J. (2001) Geochemistry of the Xining, Xifeng and Jixian sections, Loess Plateau of China: eolian dust provenance and paleosol evolution during the last 140 ka. *Chemical Geology* 178, 71-94. https://doi.org/10.1016/S0009-2541(00)00430-7

John, T., Scambelluri, M., Frische, M., Barnes, J.D., Bach, W. (2011) Dehydration of subducting serpentinite: implications for halogen mobility in subduction zones and the deep halogen cycle. *Earth and Planetary Science Letters* 308, 65-76. https://doi.org/10.1016/j.epsl.2011.05.038

Jovanovič, M., Gaudenyi, T., O'Hara-Dhand, K., Smalley, I. (2014) Karl Caesar von Leonhard (1779–1862), and the beginnings of loess research in the Rhine valley. *Quaternary International* 334, 4-9. https://doi.org/10.1016/j.quaint.2013.02.003

Kendrick, M.A., D'Andres, J., Holden, P., Ireland, T. (2018) Halogens (F, Cl, Br, I) in thirteen USGS, GSJ and NIST international rock and glass reference materials. *Geostandards and Geoanalytical Research* 42, 499-511. https://doi.org/10.1111/ggr.12229

Li, Y., Song, Y., Yan, L., Chen, T., An, Z. (2015) Timing and spatial distribution of loess in Xinjiang, NW China. *PLoS One* 10, e0125492. https://doi.org/10.1371/journal.pone.0125492

Marks, M.A., Kendrick, M.A., Eby, G.N., Zack, T., Wenzel, T. (2017) The F, Cl, Br and I Contents of Reference Glasses BHVO-2G, BIR-1G, BCR-2G, GSD-1G, GSE-1G, NIST SRM 610 and NIST SRM 612. *Geostandards and Geoanalytical Research* 41, 107-122. https://doi.org/10.1111/ggr.12128

Martignier, L., Nussbaumer, M., Adatte, T., Gobat, J.-M., Verrecchia, E.P. (2015) Assessment of a locally-sourced loess system in Europe: The Swiss Jura Mountains. *Aeolian Research* 18, 11-21. https://doi.org/10.1016/j.aeolia.2015.05.003

Mayer, L.M., Schick, L.L., Allison, M.A., Ruttenberg, K.C., Bentley, S.J. (2007) Marine vs. terrigenous organic matter in Louisiana coastal sediments: The uses of bromine: organic carbon ratios. *Marine Chemistry* 107, 244-254. https://doi.org/10.1016/j.marchem.2007.07.007

McLennan, S.M. (1993) Weathering and Global Denudation. *The Journal of Geology* 101, 295-303. https://doi.org/10.1086/648222

Nesbitt, H., Young, G. (1982) Early Proterozoic climates and plate motions inferred from major element chemistry of lutites. *Nature* 299, 715-717. https://doi.org/10.1038/299715a0

Park, J.-W., Hu, Z., Gao, S., Campbell, I.H., Gong, H. (2012) Platinum group element abundances in the upper continental crust revisited–New constraints from analyses of Chinese loess. *Geochimica et Cosmochimica Acta* 93, 63-76. https://doi.org/10.1016/j.gca.2012.06.026

Rodbell, D.T., Forman, S.L., Pierson, J., Lynn, W.C. (1997) Stratigraphy and chronology of Mississippi Valley loess in western Tennessee. *Geological Society of America Bulletin* 109, 1134-1148. https://doi.org/10.1130/0016-7606(1997)109%3C1134:SACOMV%3E2.3.CO;2

Sayago, J.M. (1995) The Argentine neotropical loess: an overview. *Quaternary Science Reviews* 14, 755-766. https://doi.org/10.1016/0277-3791(95)00050-X

Schellenberger, A., Veit, H. (2006) Pedostratigraphy and pedological and geochemical characterization of Las Carreras loess–paleosol sequence, Valle de Tafí, NW-Argentina. *Quaternary Science Reviews* 25, 811-831. https://doi.org/10.1016/j.quascirev.2005.07.011

Schulze, T., Schwahn, L., Fülling, A., Zeeden, C., Preusser, F., Sprafke, T. (2022) Investigating the loess–palaeosol sequence of Bahlingen-Schönenberg (Kaiserstuhl), southwestern Germany, using a multi-methodological approach. *E&G Quaternary Science Journal* 71, 145-162. https://doi.org/10.5194/egqsj-71-145-2022

Sun, D., Liu, D., Chen, M., An, Z., John, S. (1997) Magnetostratigraphy and palaeoclimate of red clay sequences from Chinese Loess Plateau. *Science in China Series D: Earth Sciences* 40, 337-343. https://doi.org/10.1007/BF02877564

Sun, D., Shaw, J., An, Z., Cheng, M., Yue, L. (1998) Magnetostratigraphy and paleoclimatic interpretation of a continuous 7.2 Ma Late Cenozoic eolian sediments from the Chinese Loess Plateau. *Geophysical Research Letters* 25, 85-88. https://doi.org/10.1029/97GL03353

Wang, H., Follmer, L.R., Liu, J.C.-l. (2000) Isotope evidence of paleo–El Niño–Southern Oscillation cycles in loess-paleosol record in the central United States. *Geology* 28, 771-774. https://doi.org/10.1130/0091-7613(2000)28<771:IEOPNO>2.0.CO;2

Xiao, G., Dai, G., Tian, S., Peng, S., Li, L., Meng, X., Yin, Q. (2023) Periodic variations of alpine glaciation and desertification of the NE Tibetan Plateau: Evidence from the loess-paleosol sequences in the Menyuan Basin. *Global and Planetary Change* 226, 104160. https://doi.org/10.1016/j.gloplacha.2023.104160

Yamasaki, S.-i., Takeda, A., Watanabe, T., Tagami, K., Uchida, S., Takata, H., Maejima, Y., Kihou, N., Tsuchiya, N. (2015) Bromine and iodine in Japanese soils determined with polarizing energy dispersive X-ray fluorescence spectrometry. *Soil Science and Plant Nutrition* 61, 751-760. https://doi.org/10.1080/00380768.2015.1054773

Yu, Y., Wang, H., Liu, X. (2012) Geochemical Characteristics of Loess Deposition since Last Interglacial at Desert Margin and Its Provenance and Climatic Implications. *Acta Sedimentologica Sinica* 30, 356-365.

Zhao, H., Lu, Y., Wang, C., Chen, J., Liu, J., Mao, H. (2010) ReOSL dating of aeolian and fluvial sediments from Nihewan Basin, northern China and its environmental application. *Quaternary Geochronology* 5, 159-163. https://doi.org/10.1016/j.quageo.2009.03.008